

Learning to Swarm with Knowledge-Based Neural Ordinary Differential Equations

Tom Z. Jiahao*, Lishuo Pan* and M. Ani Hsieh

Abstract—Understanding single-agent dynamics from collective behaviors in natural swarms is crucial for informing robot controller designs in artificial swarms and multiagent robotic systems. However, the complexity in agent-to-agent interactions and the decentralized nature of most swarms pose a significant challenge to the extraction of single-robot control laws from global behavior. In this work, we consider the important task of learning decentralized single-robot controllers based solely on the state observations of a swarm’s trajectory. We present a general framework by adopting knowledge-based neural ordinary differential equations (KNODE) – a hybrid machine learning method capable of combining artificial neural networks with known agent dynamics. Our approach distinguishes itself from most prior works in that we do not require action data for learning. We apply our framework to two different flocking swarms in 2D and 3D respectively, and demonstrate efficient training by leveraging the graphical structure of the swarms’ information network. We further show that the learnt single-robot controllers can not only reproduce flocking behavior in the original swarm but also scale to swarms with more robots.

I. INTRODUCTION

Many natural swarms exhibit mesmerizing collective behaviors [12], [3], [25], [1], and have fascinated researchers over the past decade [23]. A central question is how do these behaviors emerge from local interactions. Such fascination has led to much developments in artificial swarms and multi-agent robotic systems to emulate the swarms in nature. [13], [20], [15].

Some of the earliest works on developing swarm controllers rely heavily on physical intuitions and design controllers in a bottom-up fashion. Boids was developed by combining rules of cohesion, alignment, and separation to mimic the flocking behavior in natural swarms [13]. [24] proposed self-driven particles to investigate the emergence of collective behaviors in biologically motivated swarms. [20], [19] designed flocking controllers for fixed and dynamic network topologies with stability guarantees. These early works laid the foundation of decentralized swarm control and offered a glimpse of the myriad of possible swarm behaviors achievable using local controllers.

Related Works Modern machine learning has enabled pattern discovery from complex and high-dimensional data sets. It opens up avenues for learning swarm controllers directly from observations of the swarm itself, providing

a top-down approach to controller synthesis. Various data-driven methods have been used to model local control policy in swarms. Feedforward neural networks have been used to approximate decentralized control policies by training on the observation-action data from a global planner [14]. Furthermore, deep neural networks have been used to model higher order residual dynamics to achieve stable control in a swarm of quadrotors [17]. Recently, graph neural networks (GNN) have been extensively used in swarms, owing to their naturally distributed architecture. GNN allows efficient information propagation through networks with underlying graphical structures [22], and have been noted for their stability and permutation equivariance [4]. Decentralized GNN controllers have been trained with global control policies to imitate flocking [22]. All these works poses the controller synthesis problem as an imitation learning problem, and require knowledge of the actions resulting from an *optimal* control policy for learning or improving the local controllers. In practice, action data can be difficult to access, especially when learning behaviors from natural or adversarial swarms. In addition, GNNs can potentially allow a robot to access the state information of robots outside its communication range through information propagation. The extent of decentralization may therefore be limited when more propagation hops are allowed.

Deep reinforcement learning has also been applied to swarms for various applications [7]. Early works like [8] learn a decentralized control policy for maintaining distances within a swarm and target tracking. An inverse reinforcement learning algorithm was presented in [18] to train a decentralized policy by updating the reward function alongside the control policy based on an expert policy. In addition, GNNs have also been used within the reinforcement learning framework for learning connectivity for data distribution [21]. However, reinforcement learning is usually employed to solve task-specific problems with well-defined goals. The specific objectives of swarms may be difficult to discern from only observations, and therefore reinforcement learning is often not suitable for learning single-agent control strategies from solely observational data.

The contribution of this work is three-fold. First, we demonstrate the feasibility of learning single-robot controllers that can achieve the observed global swarming behaviors from only swarm trajectory data. Second, we propose a generalized model for incorporating known robot dynamics to facilitate learning single-robot controllers. Lastly, we show how to efficiently scale KNODE for learning from local information in a multi-agent setting.

This work was supported by ARL DCIST CRA W911NF-17-2-0181 and Office of Naval Research (ONR) Award No. 14-19-1-2253.

All authors in this work are with the GRASP Laboratory, University of Pennsylvania, Philadelphia, PA 19104, USA. {panls, zjh, m.hsieh}@seas.upenn.edu

*Equal contribution.

II. PROBLEM FORMULATION

We consider the problem of learning single-robot controllers based on the observations of the trajectory of a swarm. We assume that the swarm is homogeneous, *i.e.*, all robots in the swarm use the same controller. Given a swarm of n agents, we make m observations at sampling times $T = \{t_1, t_2, \dots, t_m\}, t_i \in \mathbb{R}$ given by

$$\begin{bmatrix} \mathbf{Z}^T(t_1) \\ \mathbf{Z}^T(t_2) \\ \vdots \\ \mathbf{Z}^T(t_m) \end{bmatrix} = \begin{bmatrix} \mathbf{z}_1(t_1) & \mathbf{z}_2(t_1) & \cdots & \mathbf{z}_n(t_1) \\ \mathbf{z}_1(t_2) & \mathbf{z}_2(t_2) & \cdots & \mathbf{z}_n(t_2) \\ \vdots & \vdots & \ddots & \vdots \\ \mathbf{z}_1(t_m) & \mathbf{z}_2(t_m) & \cdots & \mathbf{z}_n(t_m) \end{bmatrix},$$

where the matrix $\mathbf{Z}(t_i) \in \mathbb{R}^{n \times d}$ is the observations of the states of all n agents at t_i , and the vector $\mathbf{z}_i(t_j) \in \mathbb{R}^d$ is the state of agent i observed at t_j with dimension d . For instance, in a first-order system, an agent modeled as a rigid body in a 3-dimensional space has $d = 6$, where the first three dimensions correspond to the positions and the last three the orientations. Our goal is to learn a single-robot controller solely from the observations \mathbf{Z} .

The evolution of each individual robot's state can be described by the true dynamics given by

$$\dot{\mathbf{z}}_i(t) = f_i(\mathbf{z}_i, u_i), \quad (1)$$

where \mathbf{z}_i is the state of robot i , and u_i is its control law. The function $f_i(\cdot, \cdot)$ defines the dynamics given the state of robot and control law u_i . It is assumed that all robots in the swarm have the same dynamics and control strategy, and therefore we can drop the subscripts and rewrite (1) as $\dot{\mathbf{z}}_i(t) = f(\mathbf{z}_i, u)$ for all i . The control law u is a function of the states of other robots in the swarm, and defines the interaction between robot i . For example, a control law u can be designed to let each robot only interact with its neighbors within some communication radius.

The dynamics of the entire swarm can be written as a collection of the single-robot dynamics as

$$\dot{\mathbf{Z}}(t) = [\dot{\mathbf{z}}_1(t), \dot{\mathbf{z}}_2(t), \dots, \dot{\mathbf{z}}_n(t)]^T. \quad (2)$$

Given the initial conditions of all robots \mathbf{Z}_0 at t_0 , the states of all robots at t_1 is given by

$$\mathbf{Z}(t_1) = \mathbf{Z}_0 + \int_{t_0}^{t_1} \dot{\mathbf{Z}}(t) dt. \quad (3)$$

In practice, the integration in (3) is performed numerically. Our task is to find a single-robot control law parameterized by θ as part of the single-robot dynamics given by

$$\dot{\mathbf{z}}_i(t) = \hat{f}(\mathbf{z}_i, \hat{u}_\theta), \quad (4)$$

where \hat{u}_θ is the single-robot control law parameterized by θ . The learnt controller should best reproduce the observed swarm behaviors.

III. KNOWLEDGE-BASED NEURAL ORDINARY DIFFERENTIAL EQUATIONS (KNODE)

KNODE is a scientific machine learning framework that applies to a general class of dynamical systems. It has been shown to model a wide variety of systems with nonlinear and chaotic dynamics. In our problem, we assume a single-robot dynamics in the form of (4). From a dynamical systems perspective, $f(\mathbf{z}_i, \hat{u}_\theta)$ is a vector field. This makes KNODE a suitable method for our problem because it directly models vector fields using neural networks [9]. To put KNODE in the context of our learning problem, given some known swarm dynamics $\tilde{f}(\mathbf{Z})$ as knowledge, KNODE optimizes for the control law as part of a dynamics given by

$$\dot{\mathbf{z}}_i(t) = \hat{f}(\mathbf{z}_i, \hat{u}_\theta, \tilde{f}(\mathbf{Z})), \quad (5)$$

where the control law \hat{u}_θ is a neural network, and \hat{f} defines the coupling between the knowledge and the rest of the dynamics. While the original KNODE linearly couples a neural network with \tilde{f} using a trainable matrix \mathbf{M}_{out} [9], we note that the way knowledge gets incorporated is flexible. In later sections we will demonstrate how to effectively incorporate knowledge for learning single-robot controllers. Furthermore, the ability to incorporate knowledge will require less training data [10], [9].

We minimize the mean squared error (MSE) between the observed trajectories and the trajectories predicted from the estimate dynamics using \hat{u}_θ for robot i . A loss function is given by

$$L(\theta) = \frac{1}{m-1} \sum_{j=1}^{m-1} \sum_{i=1}^n \|\hat{\mathbf{z}}_i(t_{j+1}, \mathbf{z}_i(t_j)) - \mathbf{z}_i(t_{j+1})\|^2, \quad (6)$$

where $\hat{\mathbf{z}}_i(t_{j+1}, \mathbf{z}_i(t_j))$ is the estimated state of robot i at t_{j+1} generated using the initial condition $\mathbf{z}_i(t_j)$ at t_j , and it's given by

$$\hat{\mathbf{z}}_i(t_{j+1}, \mathbf{z}_i(t_j)) = \mathbf{z}_i(t_j) + \int_{t_j}^{t_{j+1}} \hat{f}(\mathbf{z}_i, \hat{u}_\theta, \tilde{f}(\mathbf{Z})) dt. \quad (7)$$

Intuitively, the loss function in (6) computes the one-step-ahead estimated state of all robots from every snapshot in the observed trajectory, and then computes the average MSE between the estimated and observed states for the entire trajectory from t_1 to t_{m-1} .

Our learning task can then be formulated as an optimization problem given by

$$\min_{\theta} L(\theta), \quad (8)$$

$$\text{s.t. } \dot{\mathbf{z}}_i = \hat{f}(\mathbf{z}_i, \hat{u}_\theta, \tilde{f}(\mathbf{Z})), \text{ for all } i, \quad (9)$$

which includes the dynamics constraint for all robots in the swarm. The parameters θ can then be estimated by $\theta = \arg \min_{\theta} L(\theta)$. The gradients of θ with respect to the loss can be computed by either the conventional backpropagation or the adjoint sensitivity method. The adjoint sensitivity method has been noted as a more memory efficient approach than backpropagation, though at the cost of training speed [5]. In this work, we use the adjoint method for training similar to that in [2] and [9].

IV. METHOD

In this section, we walk through the process to construct $\hat{f}(\mathbf{z}_i, \hat{u}_\theta)$ in the context of learning to swarm and the incorporation of knowledge in the form of known single robot dynamics.

A. Decentralized Information Network

We assume a robot in a swarm can only use its local information as inputs to its controller. To incorporate this assumption, we impose a decentralized information network on the swarm. Specifically, we assume robots have finite communication ranges and can only communicate with a fixed number of neighbors, denoted by k , within this range. We denote the communication radius by d_{cr} . We refer to these neighbors as the *active neighbors*. If there are more than k neighbors within a robot's communication radius, only the closest k neighbors are considered to be the *active* ones.

We leverage the communication graph of the swarm to compute the local information for each robot at each time step. The communication graph at time t can be described by a *graph shift operator* $\mathbf{S}(t) \in \mathbb{R}^{n \times n}$, which is a binary adjacency matrix computed based on d_{cr} and the positions of all robots at each time step. In this work, we treat the communication radius d_{cr} as a hyperparameter. Note that the communication graph is time-varying because the information network changes as robots move around in a swarm. Then $\mathbf{S}_{ij}(t) = 1$ if the Euclidean distance between agents i and j is less than or equal to d_{cr} , and $\mathbf{S}_{ij}(t) = 0$ otherwise. The index set of the neighbors of robot i at time t is therefore given by

$$\mathcal{N}_i(t) = \{j | j \in \mathcal{I}, \mathbf{S}_{ij}(t) = 1\}, \quad (10)$$

where $\mathcal{I} = 1, \dots, n$ is the index set of all robots. Note that set of neighbors of robot i also includes itself. At time t , the information kept by robot i is the matrix $\mathbf{Y}_i(t) \in \mathbb{R}^{k \times d}$ given by

$$\mathbf{Y}_i(t) = g(\{\mathbf{z}_j(t) | j \in \mathcal{N}_i(t)\}, k), \quad (11)$$

where the function $g(\cdot, k)$ maintains the dimension of the matrix $\mathbf{Y}_i(t)$, and forms the rows of matrix $\mathbf{Y}_i(t)$ using the state information of robot i 's active neighbors in descending order of their Euclidean distance from robot i . If there are fewer than k active neighbors within a robot's communication radius, the remaining rows in $\mathbf{Y}_i(t)$ are padded with zeros. In this work, k is treated as a hyperparameter.

The matrix $\mathbf{Y}(t)$ represents the local information accessible to each robot at time t and it completes the decentralized information network of the swarm. In summary, (10) and (11) enforces the assumptions of finite communication and perception radii for each robot.

B. Information Time Delay

In addition to a decentralized information structure, we further assume that each robot only gets delayed state information from its neighboring robots by a time lag τ . This is to emulate the latency in agent communication in

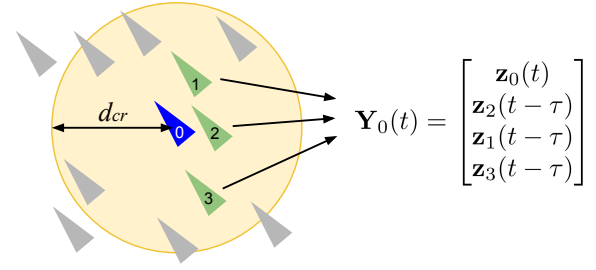


Fig. 1. Decentralized information network for robot 0 with time delay τ , and 3 active neighbors. The image shows robot 0's egocentric view, where 8 neighbors are within its communication range d_{cr} . Only the closest three neighbors contribute to the information structure of robot 0. Their states from $t - \tau$ are ordered based on their proximity to robot 0 to form $\mathbf{Y}_0(t)$.

real swarms. With time delay, the information structure of robot i in (11) becomes

$$\mathbf{Y}_i(t) = g(\{\mathbf{z}_j(t - \tau) | i \neq j, j \in \mathcal{N}_i(t - \tau)\}, k). \quad (12)$$

Fig. 1 shows an example of the information structure described by (12) using $k = 3$. The process of constructing $\mathbf{Y}_i(t)$ for all $t \in T$ in (10), (11) and (12) leverages the graphical structure of the swarm's information network. During training, the collection of delayed neighbor information is done efficiently through the matrix multiplication $\mathbf{S}(t - \tau)\mathbf{Z}(t - \tau)$, which leaves for each robot only the state information of its neighbors at $t - \tau$. Then for robot i we append the i th row of $[\mathbf{S}(t - \tau)\mathbf{Z}(t - \tau)]$ to its own state $\mathbf{z}_i(t)$. Finally we only keep k rows of the resulting matrix to form $\mathbf{Y}_i(t)$. Compared to some GNN approaches [22], [4], the information structure $\mathbf{Y}_i(t)$ in our work is more explicit. A robot with GNN controllers can only access the diffused state information from other robots, *i.e.* the neighbors' information has been repeatedly multiplied by the graph operators before reaching this robot. In this work, we directly let each robot access the state information of its active neighbors. In real-world implementation of robot swarms, our proposed information structure in (12) is more realistic as each robot can easily subscribe to or observe its neighbors' states. In addition, the information structure $\mathbf{Y}_i(t)$ enables scalable learning as we can treat the robots in a swarm as batches. As a result, training memory scales linearly with the number of robots in the swarm, and training speed scales sub-linearly.

C. Knowledge Embedding

In this work, a potential-function-based obstacle avoidance strategy similar to [11] is used as knowledge. Let the distance between robot i and an obstacle \mathcal{O} be $d_{\mathcal{O}}(\mathbf{z}_i)$, where \mathbf{z}_i is the state and includes the position of robot i . The potential function is then given by

$$U_{\mathcal{O}}(\mathbf{z}_i) = \begin{cases} \frac{\lambda}{2} \frac{1}{d_{\mathcal{O}}^2(\mathbf{z}_i)} & \text{if } d_{\mathcal{O}}(\mathbf{z}_i) \leq d_0, \\ 0 & \text{otherwise,} \end{cases} \quad (13)$$

where λ is the gain, and d_0 is the obstacle influence threshold (*i.e.* the distance within which the potential function becomes

active). Based on this potential function, the repulsive force to avoid the obstacle \mathcal{O} is given by

$$F_{\mathcal{O}}(\mathbf{z}_i) = \begin{cases} -\nabla U_{\mathcal{O}}(\mathbf{z}_i) & \text{if } d_{\mathcal{O}}(\mathbf{z}_i) \leq d_0, \\ 0 & \text{otherwise,} \end{cases} \quad (14)$$

When multiple obstacles are present, the repulsive forces computed from each obstacle are summed for a resultant repulsive force. For collision avoidance, we assume that each agent will only actively avoid its closest neighbor within d_0 at any given time.

Assuming that the robots in a swarm follow first-order dynamics, we combine the decentralized information network in (11) and the knowledge in (14) into a dynamics given by

$$\dot{\mathbf{z}}_i = \hat{f}(\mathbf{z}_i, \hat{u}_{\theta}(\mathbf{Y}_i, \mathbf{z}_i)) - \sum_j \lambda_j \nabla U_{\mathcal{O}_j}(\mathbf{z}_i), \quad (15)$$

where u_{θ} is a neural network, and λ_j is a trainable gain for avoiding obstacle \mathcal{O}_j . Both u_{θ} and λ_j are trained using the KNODE framework. Note that since all robots in a homogeneous swarm share the same control law, the training is done in batches of robots to accelerate training.

V. LEARNING TO FLOCK IN 2D

We use a global controller proposed by [20] to generate observations for our learning problem.

A. Simulation in 2D and training

This global controller achieves stable flocking, which ensures eventual velocity alignment, collision avoidance and group cohesion in a swarm of robots. The robots follow the double integrator dynamics given by

$$\begin{aligned} \dot{\mathbf{r}}_i &= \mathbf{v}_i, \\ \dot{\mathbf{v}}_i &= \mathbf{u}_i, \quad i = 1, \dots, n, \end{aligned} \quad (16)$$

where \mathbf{r}_i is the 2D position vector of robot i , \mathbf{v}_i is its velocity vector. The full state of each robot is therefore $\mathbf{x} = [\mathbf{r}, \mathbf{v}] \in \mathbb{R}^4$. The control law \mathbf{u}_i is given by

$$\mathbf{u}_i = - \sum_{j \in \mathcal{N}_i} (\mathbf{v}_i - \mathbf{v}_j) - \sum_{j \in \mathcal{N}_i} \nabla_{\mathbf{r}_i} V_{ij}, \quad (17)$$

where V_{ij} is a differentiable, nonnegative, and radially unbounded function of the distance between robot i and j [20]. The first summation term in (17) aims to align the velocity vector of robot i with those of its flockmates, while the second summation term is the total potential field around robot i responsible for both collision avoidance and cohesion [20]. The set \mathcal{N}_i is the set of all robots in the swarm for the global controller.

We use the 4th order Runge-Kutta method to simulate the dynamics in (17) with a step size of 0.01. The locations of robots are initialized uniformly on a disk with radius \sqrt{n} to normalize the density within the swarm. The velocities of robots are initialized uniformly with magnitudes between [0, 3]. Additionally, a uniformly sampled velocity bias with magnitude between [0, 3] is added to the swarm. A total of 35 trajectories are simulated, each with a total of 2000 steps.

The lengths of the trajectories is chosen such that the swarms will converge to stable flocking. We use 30 trajectories as the training data, and the remaining 5 as the testing data. We added zero-mean Gaussian noise with variance 0.001 to the training trajectories. This is known as *stabilization noise* in modeling dynamical systems and has been shown to improve model convergence [26].

The training model follows (15). There are no obstacles to avoid in the 2D case, so the potential function is only used to avoid collision among the agents. Specifically, we let each robot avoid its closest neighbor at every time step. For the controller \hat{u}_{θ} , we use a one layer neural network with 128 hidden units, and a hyperbolic tangent activation function. The trainable gain for collision avoidance is defined as $\lambda = a + \phi^2$, where a is a positive number for setting the minimum amount of force to avoid collision. The single parameter ϕ is trained together with the neural network to provide more forces for collision avoidance as needed. We do not assume information delay in the 2D case.

B. Evaluating flocking in 2D

We evaluate flocking behavior using two metrics:

Average velocity difference (*avd*) measures how well the velocities of robots are aligned in 2D flocking. It is given by

$$avd(t) = \frac{2}{n(n-1)} \sum_{i \neq j} \|\mathbf{v}_i(t) - \mathbf{v}_j(t)\|_2. \quad (18)$$

Average minimum distance to a neighbor (*amd*) measures the cohesion between agents in both 2D and 3D when flocking is achieved. It is given by

$$amd(t) = \frac{1}{n} \sum_{i=1}^n \min_j \|\mathbf{r}_i(t) - \mathbf{r}_j(t)\|_2. \quad (19)$$

amd should decrease as the robots move closer together, but it should not reach zero if collision avoidance is in place.

C. 2D Results

Fig. 2 shows 4 snapshots of one swarm trajectory generated using the trained single-robot controller. The communication radius is 5 and the number of active neighbors is 6. The robots in the snapshots are initialized using the initial states from one of the testing trajectories. It can be observed that at around $t = 600$, the predicted robots have mostly aligned their velocities in the same direction, indicating the emergence of flocking behavior. This can be further verified by the metrics for 2D flocking as shown in Fig. 3. The predicted swarm follow similar trends as the ground truth under both metrics. Furthermore, we deployed the trained controller on a larger swarm with 100 agents. Fig. 4 shows that the learnt controller generalizes to swarms with more agents and flocking emerges after about 800 steps. We do note that with some initialization, the 100-agent swarm tends to split into subswarms. This is not unexpected since stability of the original controller is only guaranteed under certain conditions [20], [19].

VI. LEARNING TO FLOCK IN 3D

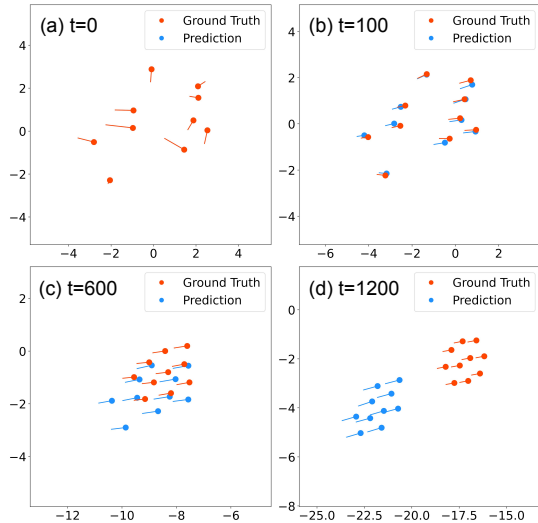


Fig. 2. Predicted trajectory of 10 robots using the learnt controller ($d_{cr} = 5, k = 6$) with the same initial states as the testing data. The subfigures (a)(b)(c)(d) show the snapshots of the swarm at $t = 0, 100, 600,$ and 1200 respectively.

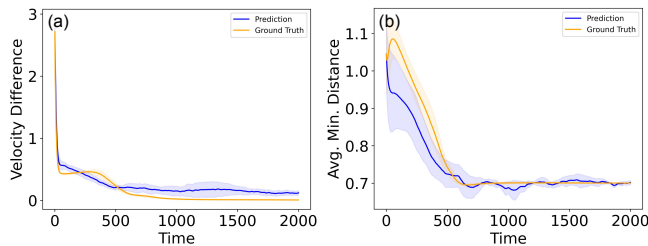


Fig. 3. The metrics for the learnt 2D controller ($d_{cr} = 5, k = 6$) show (a) average velocity difference, and (b) average minimum distance to a neighbor. The 95% confidence intervals are based on 5 sets of testing trajectories.

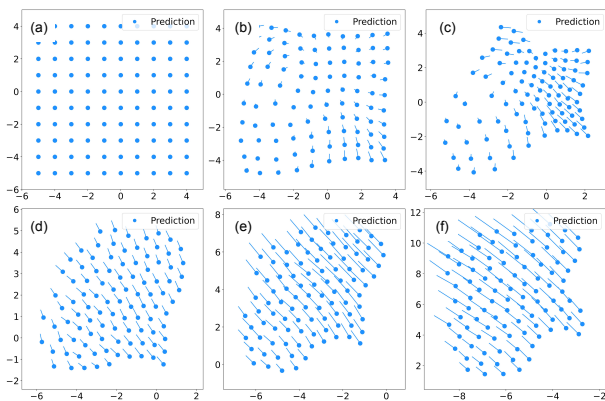


Fig. 4. Predicted trajectory of 100 robots using the learnt controller ($d_{cr} = 5, k = 6$) with uniformly initialized positions and zero velocities. The subfigures (a)(b)(c)(d)(e)(f) show the snapshots of the swarm at $t = 0, 200, 400, 800, 1000$ and 1200 respectively.

Next, we apply our learning method on the 3D simulation of boids. Boids were introduced to emulate flocking behaviors and led to the creation of *artificial life* in the field of computer graphics [13]. The flocking behavior of boids is more challenging to learn because their steady state flocking behavior is more complex than the 2D flocking in the previous section when the swarm is confined within limited volume.

A. Simulation in 3D and training

Boids are simulated based on three rules:

- **cohesion** each boid moves towards the average position of its neighboring boids.
- **alignment** each boid steer towards the average heading of its neighboring boids.
- **separation** each boid steer towards direction with no obstacles to avoid colliding into its neighboring boids.

While cohesion and collision avoidance are grouped into one term in the 2D flocking case, boids use two separate terms. Furthermore, the boids in simulation are confined in a cubic space and are tasked to avoid the boundaries.

Boids are simulated in Unity [16]. We follow the default settings with a minimum boids speed of 2.0, a maximum speed of 5.0, a communication range of 2.5, a collision avoidance range of 1.0, a maximum steering force of 3.0, and the weights of cohesion, alignment, and separation steering force are all set to 1.0. For obstacle avoidance we set the scout sphere radius as 0.27, the maximum search distance as 5.0, and the weight of obstacle avoidance steering force as 10.0. Boids are simulated in a cubic space with an equal side length of 10, with each axis ranging from -5 to 5 . The boids' positions are randomly initialized within a sphere of radius 5 centered at origin, and their velocities vectors are randomly initialized with a constant magnitude.

Unity can log both the positions and velocities of boids. However, to make the learning task more challenging, we normalize the velocities before including them in the training data, *i.e.*, only the positions and orientation of the boids are given. For a swarm of 10 boids we simulate 6 trajectories, each with a total of 1700 steps. We discard the first 10 time steps to remove simulation artifacts (There are 'jumps' in the first few steps of simulation) and only use the remaining 1690 steps. We use 2 trajectories for training and the remaining 4 as the testing data. Zero-mean Gaussian noise with variance 0.01 is added to the training trajectories.

The training model follows (15). The controller \hat{u}_θ uses a one layer neural network with 128 hidden units and a hyperbolic tangent activation function. In addition to collision avoidance, we also avoid the boundaries of the cubic space. This is implemented by avoiding the closest three points on the boundaries in the three axes at any given time. Collision and obstacle avoidance use different trained gains, both of which are defined as $\lambda = \phi^2$. We further assume an information delay of 1.

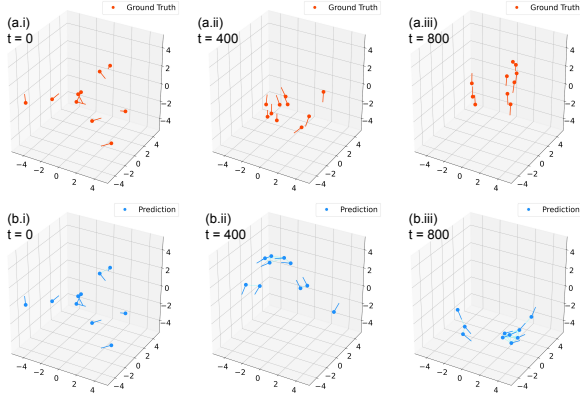


Fig. 5. Ground truth and predicted trajectories of 10 robots using the learnt controller ($d_{cr} = 2, k = 6$). The subfigures (a.i)(a.ii)(a.iii) show snapshots of the ground truth trajectory at $t = 0, 400, 800$, and (b.i)(b.ii)(b.iii) show the eventual flocking and the formation process of subswarms at $t = 0, 400, 800$. The light blue lines connect the neighbors in the swarm.

B. Evaluating flocking in 3D

Average minimum distance to a neighbor from (19) is also used for 3D flocking to measure the cohesion between robots. However, average velocity difference is not a good metric for evaluating flocking in 3D for two reasons: (1) boids only align their velocity with the local flockmates because of the presence of obstacles, and (2) boids form subswarms. As a result, velocity alignment is often not achievable at steady state flocking in boids. We instead compare the **Proper orthogonal decomposition (POD) modes** of the true and predicted trajectory to check how similar the energy distributions are in their respective dynamics. POD is a model order reduction technique which decomposes the trajectory of a system into modes based on their *energy* [6]. Systems with similar dynamics should have similar distributions of POD modes.

C. 3D Results

Fig. 5 shows the testing data and the swarm trajectories generated using the learnt controller. It uses a communication radius of 2 and the number of active neighbors is 6. The robots are initialized using the same initial states as the testing trajectory. The predicted trajectories shows the formation of subswarms during steady state flocking similar to that of the testing trajectory. Note that when the robots are initialized closer to each other, they are more likely to form a single swarm during steady state flocking. The metrics for the learnt controller are shown in Fig. 6. It can be seen that group cohesion is achieved as both the predicted and true swarm show similar trends for *amd*. Furthermore, the distributions of POD modes between the prediction and testing data are similar. This indicates the learnt controller gives the swarm a similar dynamics as the ground truth. Lastly, we apply the learnt controller on a larger swarm with 50 agents. Fig. 7 shows the emergence of flocking behavior at about $t = 400$.

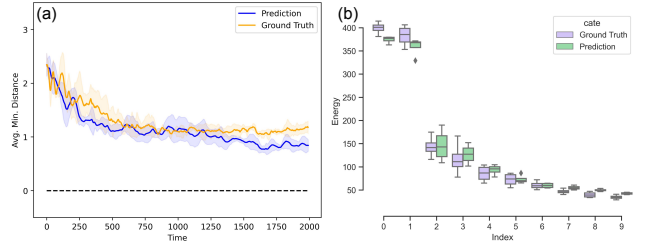


Fig. 6. The metrics for the learnt 3D controller ($d_{cr} = 2, k = 6$). (a) Average velocity difference in the predicted trajectory converges, and (b) the distribution of the first 10 POD modes of the predictions and ground truth are similar. The 95% confidence intervals are based on 4 sets of testing trajectories.

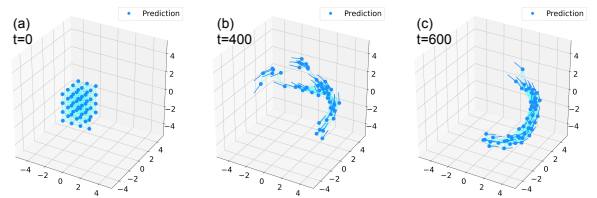


Fig. 7. The flocking of 50 robots using the learnt controller ($d_{cr} = 2, k = 6$) with uniformly initialized positions and zero velocities. The subfigures (a)(b)(c) show the snapshots of the swarm at $t = 0, 400, 600$ respectively. The light blue lines connect the neighbors in the swarm.

VII. DISCUSSION

Our experiments show that the model proposed in (15) is able to learn flocking in both 2D and 3D. We treated the communication radius d_{cr} and the number of active neighbors k as hyperparameters that need to be tuned during training. The choices of d_{cr} and k and the corresponding learnt controllers can inform how the extent of decentralization can affect flocking behavior in robot swarms. We perform a grid search using different d_{cr} and k for 2D flocking. To evaluate the performance of flocking in 2D in the grid search, we use a single number metric, namely the velocity variance which is given by

$$C = \frac{1}{n} \sum_{i=1}^m \sum_{j=1}^n \left\| \mathbf{v}_j(t_i) - \frac{1}{n} \left[\sum_{k=1}^n \mathbf{v}_k(t_i) \right] \right\|^2. \quad (20)$$

This metric measures the spread of robot velocities throughout time. It should be small if robots reach consensus in their velocities. Fig. 8 shows the grid search result. We observe that for small proximity radii or small number of active neighbors, the velocity variance tends to be large. This matches our intuition as a small d_{cr} or k means that each robot can communicate with fewer neighbors and therefore has less information to act upon in order to stay connected and flock as a swarm.

VIII. CONCLUSION AND FUTURE WORK

We have introduced an effective machine learning algorithm for learning to swarm. Specifically, we applied the algorithm to two different flocking swarms in 2D and 3D respectively. In both cases, the learnt controllers are able

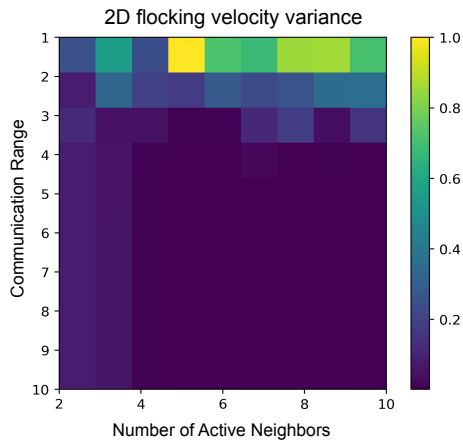


Fig. 8. Grid search on the velocity variance using different communication radius and number of active neighbors. Small communication radius and small number of active neighbors show poor velocity convergence as expected.

to reproduce flocking behavior similar to the ground truth. Furthermore, the learnt controllers can scale to larger swarms to produce flocking behaviors. We have shown the effectiveness of knowledge embedding in learning decentralized controllers, and demonstrated the feasibility of learning swarm behaviors from state observations alone, distinguishing our work from prior works on imitation learning. For future work, we plan to implement the learnt controllers on physical robot platforms to emulate swarming behaviors. In addition, we hope to employ neural networks with special properties to derive stability guarantees for the learnt controllers.

REFERENCES

- [1] C. M. Breder. Equations descriptive of fish schools and other animal aggregations. *Ecology*, 35(3):361–370, 1954.
- [2] Tian Qi Chen, Yulia Rubanova, Jesse Bettencourt, and David Duvenaud. Neural ordinary differential equations. In Samy Bengio, Hanna M. Wallach, Hugo Larochelle, Kristen Grauman, Nicolò Cesa-Bianchi, and Roman Garnett, editors, *NeurIPS*, pages 6572–6583, 2018.
- [3] G Flierl, D Grünbaum, S Levins, and D Olson. From individuals to aggregations: the interplay between behavior and physics. *J. Theor. Biol.*, 196(4):397–454, February 1999.
- [4] Fernando Gama, Ekaterina Tolstaya, and Alejandro Ribeiro. Graph neural networks for decentralized controllers. In *ICASSP 2021-2021 IEEE Int. Conf. on Acoust., Speech and Signal Process.*, pages 5260–5264. IEEE, 2021.
- [5] Ramin Hasani, Mathias Lechner, Alexander Amini, Daniela Rus, and Radu Grosu. Liquid time-constant networks. *arXiv preprint arXiv:2006.04439*, 2020.
- [6] Philip Holmes, John L. Lumley, and Gal Berkooz. *Turbulence, Coherent Structures, Dynamical Systems and Symmetry*. Cambridge Monographs on Mechanics. Cambridge University Press, 1996.
- [7] Maximilian Hüttenrauch, Sosc Adrian, Gerhard Neumann, et al. Deep reinforcement learning for swarm systems. *J. of Mach. Learn. Research*, 20(54):1–31, 2019.
- [8] Maximilian Hüttenrauch, Adrian Šošić, and Gerhard Neumann. Guided deep reinforcement learning for swarm systems. *arXiv preprint arXiv:1709.06011*, 2017.
- [9] Tom Z. Jiahao, M. Ani Hsieh, and Eric Forgoston. Knowledge-based learning of nonlinear dynamics and chaos. *arXiv preprint arXiv:2010.03415*, 2021.
- [10] George Em Karniadakis, Ioannis G. Kevrekidis, Lu Lu, Paris Perdikaris, Sifan Wang, and Liu Yang. Physics-informed machine learning. *Nature Reviews Physics*, 3:422–440, 06 2021.

- [11] Oussama Khatib. Real-time obstacle avoidance for manipulators and mobile robots. *The Int. J. of Robot. Res.*, 5(1):90–98, 1986.
- [12] Akira Okubo. Dynamical aspects of animal grouping: Swarms, schools, flocks, and herds. *Advances in Biophysics*, 22:1–94, 1986.
- [13] Craig W Reynolds. Flocks, herds and schools: A distributed behavioral model. In *Proc. of the 14th annual conf. on Comput. graphics and interactive tech.*, pages 25–34, 1987.
- [14] Benjamin Riviere, Wolfgang Honig, Yisong Yue, and Soon-Jo Chung. Glas: Global-to-local safe autonomy synthesis for multi-robot motion planning with end-to-end learning. *IEEE Robot. and Automat. Lett.*, 5(3):4249–4256, Jul 2020.
- [15] Michael Rubenstein, Alejandro Cornejo, and Radhika Nagpal. Robotics. programmable self-assembly in a thousand-robot swarm. *Science (New York, N.Y.)*, 345:795–9, 08 2014.
- [16] SebLague. Boids. <https://github.com/SebLague/Boids/tree/master>, 2019.
- [17] Guanya Shi, Wolfgang Hönig, Yisong Yue, and Soon-Jo Chung. Neural-swarm: Decentralized close-proximity multirotor control using learned interactions. In *2020 IEEE Int. Conf. on Robot. and Automat.*, pages 3241–3247. IEEE, 2020.
- [18] Adrian Šošić, Wasiur R KhudaBukhsh, Abdelhak M Zoubir, and Heinz Koepl. Inverse reinforcement learning in swarm systems. *arXiv preprint arXiv:1602.05450*, 2016.
- [19] Herbert Tanner, Ali Jadbabaie, and George Pappas. Stable flocking of mobile agents, part ii: Dynamic topology. *Departmental Papers (ESE)*, 2, 05 2003.
- [20] Herbert G Tanner, Ali Jadbabaie, and George J Pappas. Stable flocking of mobile agents, part i: Fixed topology. In *42nd IEEE Int. Conf. on Decision and Control*, volume 2, pages 2010–2015. IEEE, 2003.
- [21] Ekaterina Tolstaya, Landon Butler, Daniel Mox, James Paulos, Vijay Kumar, and Alejandro Ribeiro. Learning connectivity for data distribution in robot teams. *arXiv preprint arXiv:2103.05091*, 2021.
- [22] Ekaterina Tolstaya, Fernando Gama, James Paulos, George Pappas, Vijay Kumar, and Alejandro Ribeiro. Learning decentralized controllers for robot swarms with graph neural networks. In *Conf. on Robot Learn.*, pages 671–682. PMLR, 2020.
- [23] T. Vicsek. A question of scale. *Nature*, 411:421–421, 2001.
- [24] Tamás Vicsek, András Czirók, Eshel Ben-Jacob, Inon Cohen, and Ofer Shochet. Novel type of phase transition in a system of self-driven particles. *Phys. Rev. Lett.*, 75:1226–1229, Aug 1995.
- [25] K Warburton and J Lazarus. Tendency-distance models of social cohesion in animal groups. *J. Theor. Biol.*, 150(4):473–488, June 1991.
- [26] Alexander Wikner, Jaideep Pathak, Brian Hunt, Michelle Girvan, Troy Arcomano, Istvan Szunyogh, Andrew Pomerance, and Edward Ott. Combining machine learning with knowledge-based modeling for scalable forecasting and subgrid-scale closure of large, complex, spatiotemporal systems. *Chaos*, 30:053111, 05 2020.